Photolysis of Matrix-Isolated Allenylketene: An Experimental and Theoretical Study of the Allenylcarbene Reactivity

Jean-Pierre Aycard,*,† Alain Allouche,† Michèle Cossu,† and Mihaela Hillebrand‡

UMR CNRS 6633, Physique des Interactions Ioniques et Moléculaires, Equipe Spectrométries et Dynamique Moléculaire, FR W1739, Université de Provence, Case 542, 13397 Marseille Cedex 20, France, and Department of Physical Chemistry, University of Bucharest, Bdul Republicii, Bucharest, RO-7034, Romania

Received: April 22, 1999; In Final Form: September 8, 1999

The photolysis ($\lambda \geq 230$ nm) of 3,4-pentadienoyl chloride **1** isolated in argon matrix at 10 K as well as the follow-up reactions were studied by FTIR spectroscopy. The experimental data point out that the first step in the photochemical reaction is the elimination of HCl and the formation of an intermediate product identified as allenyl ketene **2**. Further irradiation determines the decarbonylation of **2** leading to a very reactive carbenic species, allenylcarbene **3**, which undergoes subsequent reactions. The final products identified were vinylacetylene **4** and acetylene **7**. The assignment of the intermediates and final products as well as the reaction mechanism is supported by high-level theoretical calculations, LSDA/6-31G** and CASSCF/6-31G*.

Introduction

Since their discovery over 100 years ago, there has been considerable interest in the determination of the reactivity and structure of carbenes.[1] These compounds are highly reactive divalent carbon intermediates that play an important role in organic chemistry. Part of this interest in carbenes arises from the fact they have two generally accessible electronic states, the singlet with all its electrons paired and the triplet with two unpaired electrons. For the simplest carbene, methylene, the singlet−triplet splitting is only 9.05 kcal mol^{-1} with a triplet ground state.[2] Carbene undergoes addition to double bonds and intramolecular rearrangements. In the latter case, a hydrogen or carbon atom will migrate to the carbenic carbon and restore its electron octet.

Conjugated carbenes, obtained by conjugation of carbene with a flanking π system, feature a delocalized system, the structure of which is more ambiguous. Vinylcarbenes[3] such as CH_2═CH−CH**:** may be formulated as derivatives of allyl-1,3-diyl ·CH_2−CH═CH·. In this case, rotation of the 3 carbon and its two pendant groups removes the allylic conjugation. This loss of conjugation would energetically be costly were it not for the compensation of 1,3 bonding. Forming a complete 1,3 bond results in a species recognized as a cyclopropene, with a highly strained C═C bond, but in fact more stable than vinylcarbenes.[4]

The isomeric C_3H_2 carbenes and C_5H_2 carbenes play an important role in interstellar space chemistry.[5] For C_3H_2, three forms have been identified in the laboratory: propynylidene, propadienylidene, and cyclopropenylidene. For propynylidene, identified in an argon matrix at 12 K,[6a] the ground state is a triplet, but its geometry is even problematic. Matrix isolation experiments coupled with results of ab initio calculations suggest that the equilibrium geometry of this isomer was a 1,3-diradical with C_2 symmetry.[6c]

From computational methods based on the coupled cluster approximation, Seburg et al. show in a recent paper that the two most stable forms of C_5H_2 are linear triplet pentadienylidene and singlet ethynylcyclopropenylidene.[5d]

There have been numerous experimental and theoretical reports on the neutral C_4H_4 isomers such vinylacetylene[7] (butenyne) **4**, butatriene[8,10b,c] **6**, cyclobutadiene,[9] cyclobutyne,[10] and methylenecyclopropene[11] **5**, but it is quite surprising that little known of the structure and reactivity of allenylcarbene (butadienylidene) CH_2═C═CH−CH**:**) **3** (Scheme 1). Nevertheless, this compound may be postulated to be a possible precursor in the synthesis of the stable isomers **4**−**6**. Allenylcarbene may be obtained by photolysis of allenylketene **2**. Stable allenylketenes have been recently synthesized by the Tidwell team.[12a] The parent compound **2** has been observed previously by Chapman in a matrix at 8 K[12b] and was postulated to be an intermediate in the pyrolytic conversion of furfuryl benzoate,[12c] but it has not been observed as a long-lived species at ambient temperatures.[12]

Our group is actively involved in the study of neutral intermediates trapped in rare gas matrixes.[13] In the present study, we report the first photolysis experiments on **2** isolated in argon matrixes. This compound was obtained by a photodehydrochlorination process of 3,4-pentadienoyl chloride **1** trapped in argon matrixes as previously observed with other acyl chloride derivatives submitted to UV irradiations.[13c−e,14] Theoretical calculations were undertaken in order to compare the experimental IR spectra with the calculated ones, to assign the observed absorption of photoproducts, and to identify the different photolysis pathways.

Experimental Section

Synthesis of 3,4-Pentadienoyl Chloride 1. 3,4-Pentadienoic acid (0,02 mol), synthesized using the procedure described by Price and Patten,[15] was placed in a three-necked round-bottomed flask equipped with a magnetic stirrer, nitrogen inlet, and an addition funnel. Freshly distilled $SOCl_2$ (0.04 mol) was added dropwise over 20 min. Excess thionyl chloride is eliminated by distillation, and the residual oil is distilled at reduced pressure (22 °C at 3 mm Hg, yield = 67%).

Matrix Isolation Experiments. Before matrix deposition, 3,4-pentadienoyl chloride **1** was mixed in the gaseous phase with an excess of argon at room temperature. The relative

† Université de Provence.
‡ University of Bucharest.

10.1021/jp991329d CCC: $18.00
Published on Web 10/22/1999

SCHEME 1: Compound Formulas and Reaction Paths for 3,4-Pentadienoyl Chloride Photolysis

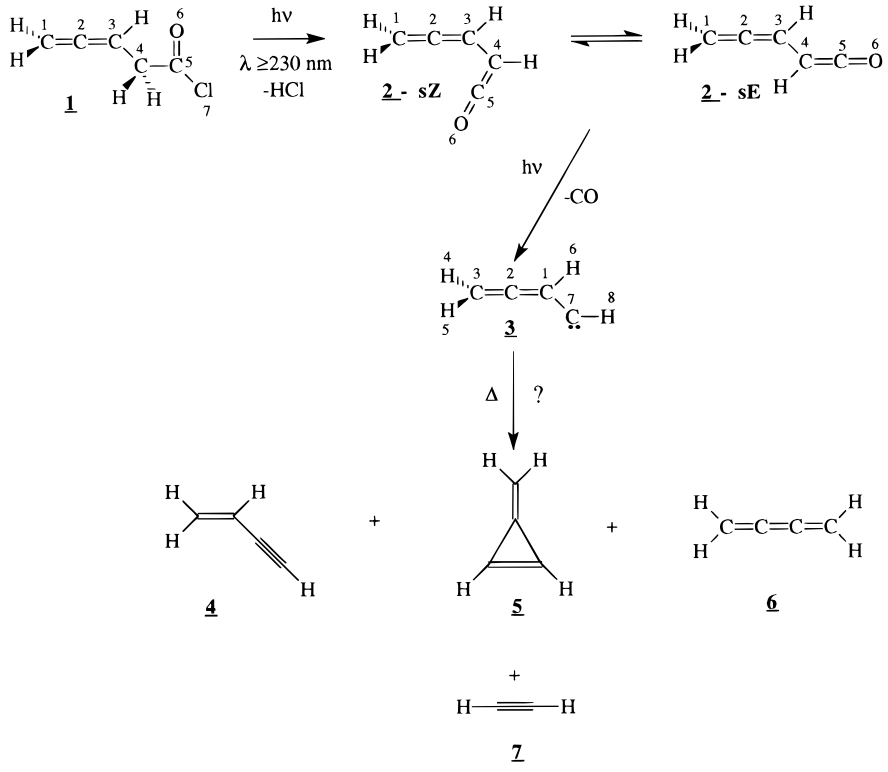

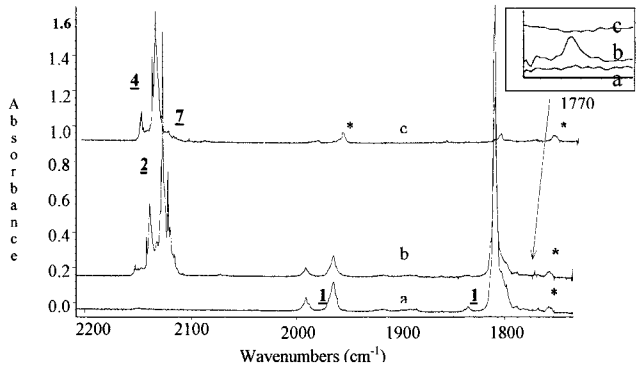

Figure 1. IR spectra, in the range 2200−1700 cm^{-1}, of the reaction mixture obtained from photolysis of **1** at t = (a) 0, (b) 130, and (c) 4600 min.* = impurities.

concentration of rare gas to 3,4-pentadienoyl chloride, at room temperature (*M*/*S* ratio = 550), was adjusted by pressure measurements; reproducible solute partial pressures required the use of a Datametrics (Barocel, series 600) capacitance manometer. The mixture was then deposited at 20 K on a CsBr window. The deposition rate of gas mixtures was controlled with an Air Liquide microleak (V.P/RX); it never exceeded 2 mmol/h, a value chosen to avoid, as far as possible, the site splitting of vibrational absorption bands. The thickness of matrixes was determined by counting transmission fringes. The matrix is cooled to 10 K before irradiation.

A concentrated matrix experiment (*M*/*S* = 200) was also performed, and the low-intensity bands are enhanced compared to the background and are therefore observable in the different compounds. In this matrix, the very strong band at 1808 cm^{-1} assigned to the stretching $\nu_{C=O}$ mode of **1** was saturated (Figure 1).

Spectroscopy Techniques. The IR spectra were recorded in the 4000−400 cm^{-1} range on a 7199 Nicolet spectrometer equipped with a liquid N_2-cooled MCT detector; the resolution was 0.12 cm^{-1} without apodization. The integrated absorbances *A* (cm^{-1}) were measured as the area under a simulated peak (giving the best fit with the experimental data) by use of the FOCAS program of the Nicolet library.

The UV spectra were recorded in the 200−800 nm range on a Unicam UV4 spectrometer.

The ^1H NMR analysis of 3,4-pentadienoyl chloride was performed on a Brüker AC200 NMR spectrometer.[16]

Irradiation Techniques. Irradiation was applied at $\lambda \geq 230$ nm using an Osram 200 W high-pressure mercury lamp equipped with a quartz envelope. The light intensity is the same in all experiments, and the irradiation area is wider than the surface used to obtain the spectrum. It is assumed that the matrix has no significant absorbance.

Computational Methods. The infrared frequencies of **2** were obtained by calculations of the ab initio force field using the Lsda approximation[17] with 6-31G** basing set.[18] The reactivity of allenylcarbene **3** and the energies of the transition states were calculated using the multiconfigurational CASSCF(6,6) method[19] implemented in the GAMESS (U. S.) computer package[20] with the 6-31G* standard basis set. The calculated total energies were not corrected for the zero-point energy (ZPE). In most of the cases, the optimized geometries were calculated using the quadratic approximation algorithm, which is a version of an augmented Hessian technique. The Schlegel quasi-Newton−Raphson method[21] was used successfully for optimization in some more difficult cases.

Results and Discussion

The photochemical behavior of the precursor **1** and the time evolution of the primary and follow-up reaction products embedded in an argon matrix are reported in Figures 1−5, where the evolution of IR spectra of the system is illustrated for three different irradiation times. The lower trace (a) presents the spectrum after deposition and before irradiation (time $t = 0$). The middle trace (b) and the upper trace (c) were taken after

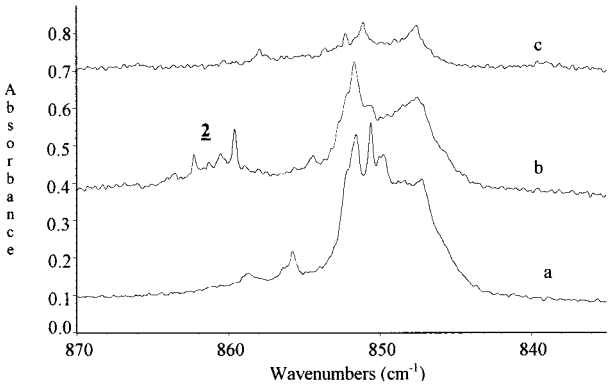

Figure 2. IR spectra, in the range 870−820 cm^{-1}, of the reaction mixture obtained from photolysis of **1** at t = (a) 0, (b) 130, and (c) 4600 min.

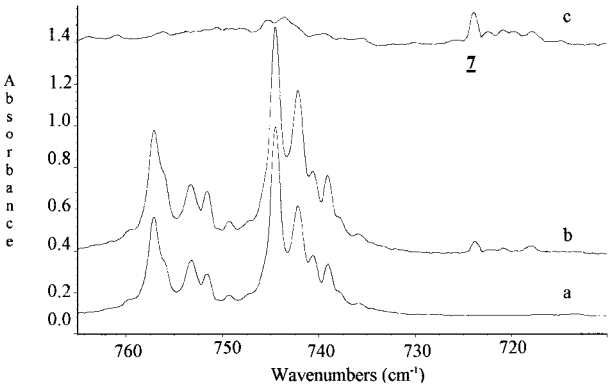

Figure 3. IR spectra, in the range 760−710 cm^{-1}, of the reaction mixture obtained from photolysis of **1** at t = (a) 0, (b) 130, and (c) 4600 min.

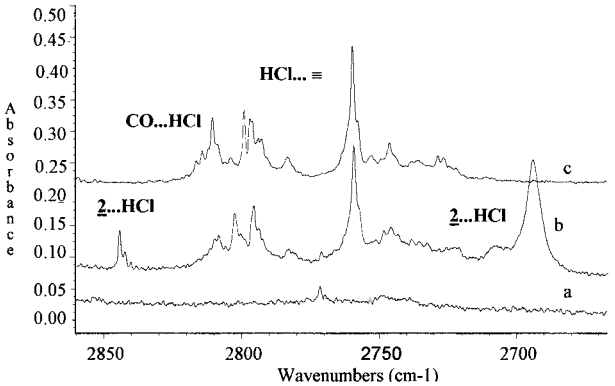

Figure 4. IR spectra, in the range 3000−3400 cm^{-1}, of the reaction mixture from photolysis of **1** at t = (a) 0, (b) 130, and (c) 4600 min.

130 and 4600 min, respectively. The experimental spectra of **2** were compared with simulated spectra. The final photoproducts were identified by comparison of their experimental spectra with literature data.[7b,e,8b,11a,c]

Infrared Spectra Analysis of 3,4-Pentadienoyl Chloride 1. The spectrum of **1**, obtained after deposition at 10 K shows the same characteristic absorption bands as those observed in the liquid phase, but with a higher resolution of the difference lines. The most characteristic features are the following. (i) A large band at 1808 cm^{-1} ($\nu_{C=O}$) and the two $\nu_{C=C=C}$ stretching modes at 1964 cm^{-1} and 1990 cm^{-1} (Figure 1). (ii) The out-of-plane mode of the terminal allene[22] in the range 830−860 with peaks at 847, 851, 852, and 856 cm^{-1} (Figure 2). The δ_{CH2} appears at 1403 cm^{-1}. (iii) A multiplet structure between 730 and 760 cm^{-1}assigned to the ν_{C-Cl} stretching mode (Figure 3).

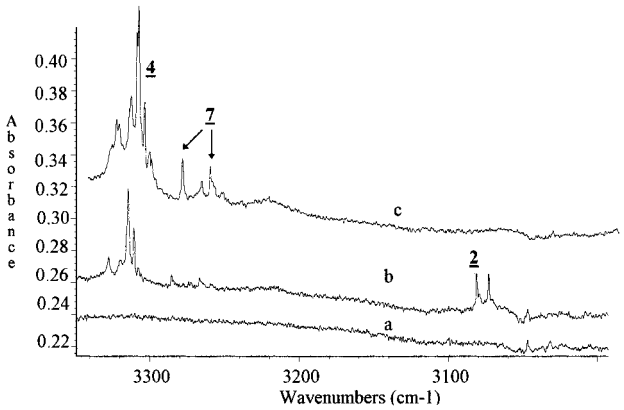

Figure 5. IR spectra, in the range 2600−2850 cm^{-1}, of the reaction mixture obtained from photolysis of **1** at t = (a) 0, (b) 130, and (c) 4600 min.

Some free HCl trapped in the argon matrix, resulting from thermal decomposition of **1**,[13d,e,23] is observed at 2870 cm^{-1}. Weak absorption bands unperturbed under irradiation or that do not show the same kinetic behavior as the **1** absorptions bands (1053−1055 and 610−613 cm^{-1}) were assigned to impurities and neglected in the foregoing discussion.

As **1** can assume several conformations by rotation around the two carbon single bonds, C_1C_2 and C_2C_3, a theoretical study of the relative stability of the different conformers was undertaken. The potential energy surface, PES, built by AM1 semiempirical methods[24] in terms of the two torsions Φ_1-($C_2C_3C_4C_5$) and Φ_2($C_3C_4C_5O_6$), reveals three local minima. Further total optimization of these minima at the Lsda/6-31G** level led to two conformers of very similar energies ΔE < 1.5 kcal mol^{-1}.

The experimental and theoretical frequencies are listed in Table 1. Multiplet structures resulting from the site effects in the matrix and the response of the different conformers are observed in most infrared bands, but the energy differences between the conformers are so minor that they rule out a possible identification of the experimental conformers spectra.

Photolysis of 1 Isolated in Argon Matrixes: Formation and Identification of Allenylketene 2. When matrix-isolated **1** was subjected to broad-band irradiation, it decomposes slowly (80% in 720 min), and new absorption bands are observed (Figures 1−5). The integrated intensities of numerous absorption bands were plotted versus time, to detect those having identical behavior to be ascribed to the same product. These evolutions of the integrated intensities of **1** and of the photoproducts under irradiation are reported in Figure 6.

The infrared spectrum, obtained after irradiation of **1**, contains the absorption bands of **2** ($s-E$ + $s-Z$), **1**, and HCl (Figures 1−5). In our experiments, several absorption bands characteristic of a ν_{HCl} stretching mode appear between 2650 and 2850 cm^{-1}, with the strongest one at 2694 cm^{-1} (Figure 5). These frequencies are lower than the value of the $R(0)$ rovibrational line observed for pure HCl trapped in rare gas cryogenic matrixes;[23] we assume that HCl is complexed with the simultaneously formed **2**. The presence of **2** is mainly supported by the appearance of a strong absorption band centered at 2127 cm^{-1} assigned to the $\nu_{C=C=O}$ stretching mode. Its first increasing and then decreasing intensity points out that **2** is an intermediate species undergoing subsequent reactions. Other bands are also in agreement with the identification of **2** as the intermediate resulting after HCl elimination; these are the following: (i) the two bands observed at 3073 and 3081 cm^{-1}, assigned to the

TABLE 1: Comparison of Experimental (argon matrix 10 K) and ab Initio Calculated Vibrational Frequencies and Relative Infrared Intensities for Compound 1

CH2=C=CH-CH2-COCl							
		theoretical (LSDA/6-31G**)					
experimental		**1a**[a]			**1b**[a]		
cm^{-1}	I^b		assignment	I^b	cm^{-1}		assignment
		3157	ν(=CH2)	<1	3156	<1	ν(=CH2)
3032	≪1	3089	ν(=CH-)	<1	3093	1	ν(=CH-)
		3076	ν(=CH2)	<1	3076	<1	ν(=CH2)
		3058	ν(CH2-)	<1	3047	<1	ν(CH2-)
2925 2905	≪1	2994	ν(CH2-)	1	2960	5	ν(CH2-)
1990	4		ν(C=C=C)[c]				ν(C=C=C)[c]
1964	12	2075	ν(C=C=C)	24	2078	23	ν(C=C=C)
(1916 1890 1884)[d,e]	1						
(*1808*)[d,f]	100	1889	ν(C=O)	100	1896	100	ν(C=O)
1443 1437	1	1437	ν(C=C=C), δ(=CH2)	4	1445	2	ν(C=C=C), δ(=CH2)
(1403)[d]	10	1383	δ(=CH2)	6	1362	12	δ(=CH2)
1348	<1	1319	δ(=CH2), δ(CCH)		1332	5	δ(=CH2), δ(CCH)
(1290 1287 1281)[d]	2	1237	δ(CCH), ν(C−C)	1	1245	12	δ(CCH), ν(C−C)
(1196 1194 1190 *1186*)[d,f]	3	1174	δ(CCH,) ν(C−C)	13	1148	2	δ(CCH), ν(C−C)
		1130	δ(CCH,) ν(C−C)	4	1122	1	δ(CCH), ν(C−C)
(1056 1052 1042 1039)[d,g]	8						
(1026 1024 1021 1019)[d]	13	1056	ν(=C−C-), ν(−C−C-)	35	1038	16	ν(=C−C-), ν(−C−C-)
(984 974 957 954 *945*)[c,f]	42	991	ν(−C−C-)	11	979	63	ν(−C−C-)
		965	δ(=C=CH2),		968	<1	δ(=C=C−H2)
		893	δ(CCH)	2	881	<1	δ(CCH)
		858	tor(=C−C-), tor(C=C)	10	845	8	tor(=C−C-), tor(C=C)
856 851 849 847)[d]	33	828	oop(=CH2)	22	828	22	oop(=CH2)
(*757* 756 753 752)[d,f]	13	666	ν(C−Cl), δ(CCO)	18	760	69	ν(C−Cl), δ(CCO)
(*746* 742 740 739)[d,f]	25						
(645 612 610)[d,g]	1,5						
(567 559 557)[d]	1	608	ν(C−Cl), δ(C=C−C)	27	571	8	δ(C=C−C), δ(CCH), tor(CC)
529−509	<1	536	tor(C=C)	6	528	2	tor (C=C), oop(CCCH)
		529	tor(C−C), tor(C=C)	2	466	<1	tor(C−C), oop(COCl)
499−486	<1	433	ν(C−Cl), δ(OCCl)	2	438	6	ν(C−Cl)
		367	δ(CCC), ν(CCl)	2	349		tor(CC)
		330			314		δ(CCCl), δ(COCl), ν(C−Cl)
		208			235		tor(CC), δ(C=C=C)
		178			146		tor(C−C)
		48			60		tor(CC)
		14			45		tor(CC)

[a] Optimized dihedral geometric parameters (for complete geometry, see Table 1S and Figure 1S): **1a** $\Phi_1 = C_2C_3C_4C5$ 117°, $\Phi_2 = C_3C_4C_5O_6$ 125°, **1b** $\Phi_1 = C_2C_3C_4C_5$ 135°, and $\Phi_2 = C_3C_4C_5O_6$ 35° [b]Experimental and theoretical integrated intensities, in percent from the strongest band. [c] From Chouteau et al.[22] [d]Absorption bands in parentheses correspond to a massif corresponding to site splitting or conformers. [e] The bands are assigned to be a harmonic of the 945 band (cf. Ramsey and Ladd[30]). [f] The strongest band is in italics. [g] Impurity.

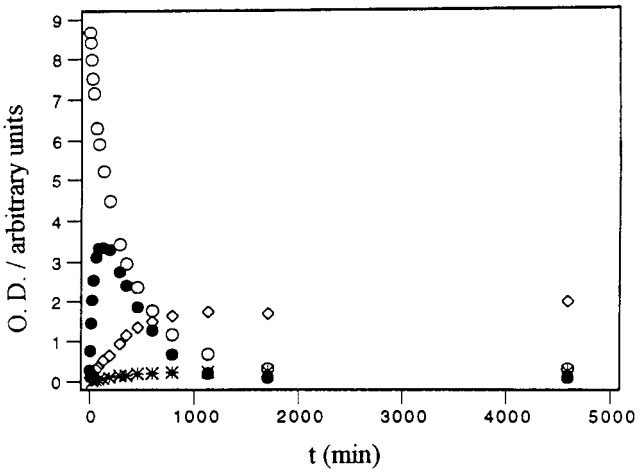

Figure 6. Plot of optical density vs time showing the evolution of the $\nu_{C=O}$ band of **1**, the formation and destruction of $\nu_{C=C=O}$ band of **2**, and of the ν_{C-H} band of the photoproducts. ○ = **1**, ● = **2**, ◇ = **4**, * = **7**.

ν_{Csp2-H} stretching modes (Figure 4); (ii) the $\nu_{C=C=C}$ stretching mode appearing in the same 1960 cm^{-1} range as those of the precursor; and (iii) the bands at 860, 861, and 862 cm^{-1} due to the $=CH_2$ out-of-plane mode appearing near the broad band of **1**, located at 850 cm^{-1}, which disappears under irradiation.

Concurrently with photolysis experiments, to collect additional information about their infrared spectra, we examined the structures and energies of **2** conformers and their connecting transition structure using ab initio molecular calculations at the LSDA/6-31G** level. As obtained by Huang et al.[12a] at the HF/6-31G* level, we found two minimum energy structures, but in our case, the *s*−*E* and the *s*−*Z* structures were found to be planar. The *s*−*E* conformer is only favored by 1.5 kcal mol^{-1} (1.1 kcal mol^{-1} in Huang et al.[12a]).

The experimental and calculated frequencies for the two possible conformers of **2**, s−E and s−Z, are collected in Table 2.

Identification of Photoproducts. After the disappearance of the absorption bands of compounds **1** and **2** (t = 4600 min), the new absorption bands observed in the infrared spectra are compared with the experimental IR spectra of the expected photoproducts: **4**,[7b] **5**,[11c] **6**,[8b] and acetylene **7**[25] (Table 3). From this comparison, the final photoproduct compounds are identified as CO, HCl, **4**, and **7** (Table 3)

TABLE 2: Comparison of Experimental (argon matrix 10 K) and ab Initio Calculated Vibrational Frequencies and Relative Infrared Intensities for *s*-E and *s*-Z Conformers of Compound 2

experimental			theoretical (LSDA/6-31G**)					
			2 *s*-E[a]			**2** *s*-Z[a]		
cm^{-1}	I^b	assignment[c]	cm^{-1}	I^b	P. E. D.[c]%	cm^{-1}	I^b	P. E. D.[c]%
3081	1.5	ν(=C−H)	3133	2	100(ν =C−H)	3143	3	100(n=C−H)
			3124		64(ν=CH2), 36 tors(C−C)	3122		84(ν=CH2), 16 tors(C−C)
			3085		100(ν=C−H)	3089		100(ν=C−H)
3073	1.5	ν(=CH2)	3052	1	100(ν=CH2)	3050	1	100(ν=CH2)
2127−2122	100	ν(C=C=O)	2234	100	100(νC=C=O)	2232	100	100(νC=C=O)
1916−1960	<1	ν(C=C=C)	2057		100(νC=C=C)	2055	1	100 (νC=C=C)
1461	1	ν(C−C)	1486	3	57(νC−C), 31(νC=C),	1453	4	47(νC−C), 29(νC=C), 18(δ=CH2)
			1383		73(δ=CH2),	1404	1	69(νC=C=O), 15(νC−C), 10(δH−CC)
			1252	1	61(δH−CC), 30(νC=C=O)	1324	1	38(δ=CH2), 41(δH−CC), 11(νC−C)
			1145	2	67(νC−C), 14(νC=C)	1140		87(δH−CC), 12 (νC=C)
			1094		72(δH−CC), 17(νC=C=O), 14(νC=C=C)	1071	1	29(δH−CC), 53(νC=C=O), 17(νC=C=C)
			1029	1	59(νC−C), 26(νC=C)	970		100(tor CC)
			969		100(δC=C=C)	899	1	78(νC−C), 21(νC=C)
			857	2	100(δC=C=C)	852	3	100(torCC)
857−862	6	oop(=CH2)	841	6	97(oop=CH2)	842	8	73(oop=CH2)
			641	2	tor(C−C)	745	4	60(δC=C=O), 35(δCCC)
632	1		603	1	95(δC=C=O)	610	2	(torC−C)
			539		89(δC=C=C)	518		39(δCCC), 56(δCCO)
			524		100(δC=C=C)	517	7	100(δC=C=C)
			476		(δC=C=C), (δC=C=O)	477	1	(δC=C=C), (δC=C=O)
			318		100(δC=C=C)	303	1	100(δC=C=C)
			231		62(δC=C=C), 30(δC=C=O)	246		67(δCCC), 31(δCCO)
			119		68(δC=C=C), 26(δC=C=O)	89		100(δC=C=C)
			88		100(δC=C=C)	88		73(δC=C=C), 20(δC=C=O)

[a] Optimized dihedral angles (for complete geometry, see Table 2S): *s*-Z $C_2C_3C_4C_5$ 0.0°; *s*-E $C_2C_3C_4C_5$ 179.96°. [b] Experimental and theoretical integrated intensities, in percent from the strongest band. [c] Key: oop = out-of-plane and tor = torsion.

TABLE 3: Experimental Vibrational Frequencies and Relative Infrared Intensity Data for Photoproducts

experiment[a]		**4**[b,c]			**7**[c,d]		
ν cm^{-1}	I^e	ν cm^{-1}	I^c	assignment	ν cm^{-1}	I	assignment
(3328,3320)	100	3330	vs	ν(C−H)			
(3316,3311)		3316	m	ν(C−H)			
3285 3265					3289	vs	ν(C≡H)
		3030	m	ν(C−H)			
1605	<1	1599	m	ν(C=C)			
		1096	m	δ(C=CH)			
1257	5	1252	s				
977	10	974	vs	oop(C≡C−H)			
928	20	927	vs	oop(CH2)			
(858 851 848)	2	874	m	ν(C−C)			
724 720 717					737	vs	δ(CCH)
		677	m	tor(C=C)			
638	15	625	vs	δ(H−C≡C)			
618	20	619	vs	δ(H−C≡C)			
		529	m	oop(C−C=C)			

[a] In argon matrix at 10 K after 4600 min; absorption bands in a massif are cited in parentheses. [b] See Tørneng et al.[7b] [c] Only very strong (vs), strong (s), and medium (m) bands are cited for clarity. Key: oop = out-of-plane and tor = torsion. [d] See Andrews et al.[25] [e] Experimental integrated intensities in percent from the strongest band.

Identification of **4** is based on the presence of the strongest bands observed in the IR spectrum of pure vinylacetylene, that is, the bands at 3300−3330 cm^{-1} (ν_{CspH}, Figure 4), 977, 928, 638, and 618 cm^{-1} (Table 3). The other possible medium- and weakly-absorbing bands are unlikely to be observed in our diluted conditions.

Acetylene, identified by two groups of absorption bands with the same kinetic behavior between 3285 and 3265 (ν_{CspH}) and between 724 and 717 cm^{-1}, is trapped with HCl in the same cage and gives **7**···HCl complexes. These complexes, previously studied by Andrews et al.,[25] are characterized by strong absorption bands at 2764 (ν_{HCl}), 3283, 752, and 737 cm^{-1}

Identification of carbon monoxide is based on the evolution of the structure of the absorption band pattern of the $\nu_{C=C=O}$ frequency range between 2200 and 2050 cm^{-1} (Figure 1). As the integrated intensities of the absorption bands were plotted against time, we are able to detect those having identical behavior indicating that they belong to the same product and hence to detect reaction products that showed different kinetic behavior. From this analysis, the decreasing and then disappearing absorption bands are attributed to **2**, and the increasing ones, between 2140 and 2154 cm^{-1}, are ascribed to free and HCl-complexed carbon monoxide trapped in argon matrix sites.

Between 2900 and 2650 cm^{-1} (Figure 5), in the ν_{HCl} area, we observe a complex spectra characterized by (i) the absorption bands corresponding to HCl/CO complex[13c,e] at 2815 cm^{-1} and (ii) the spectral response of HCl···C≡C triple bond complexes at 2759 cm^{-1}.

From theoretical studies, Tang and Cui[26] suggest three possible structures for the HCl vinylacetylene complexes. As observed experimentally by Kisiel et al.,[27] the hydrogen bond to the π electrons of a C≡C triple bond leads to a more stable complex than that for the π electrons of a C=C double bond. The most intense band at 2759 cm^{-1} could be assigned to the $\nu_{(HCl\cdots C\equiv C)}$ absorption band of a **4**···HCl or **7**···HCl complex.

During irradiation, an increasing and then decreasing very weak absorption band, which cannot be attributed to **4** or **6** is observed at 1770 cm^{-1} (Figure 1). A similar absorption band has been observed by Billups et al.[11a] in the IR spectrum of **5**. This result seems to point to the formation of methylenecyclopropene as a transient and ties in with the observations of Banert et al.[28] during irradiation of the aza analogue (2-methylene-2*H*-aziridine) generated by photolysis of azidopropadiene.

SCHEME 2: Schematic Representation of the Isomerization Reaction of Allenylcarbene Investigated in This Work[a]

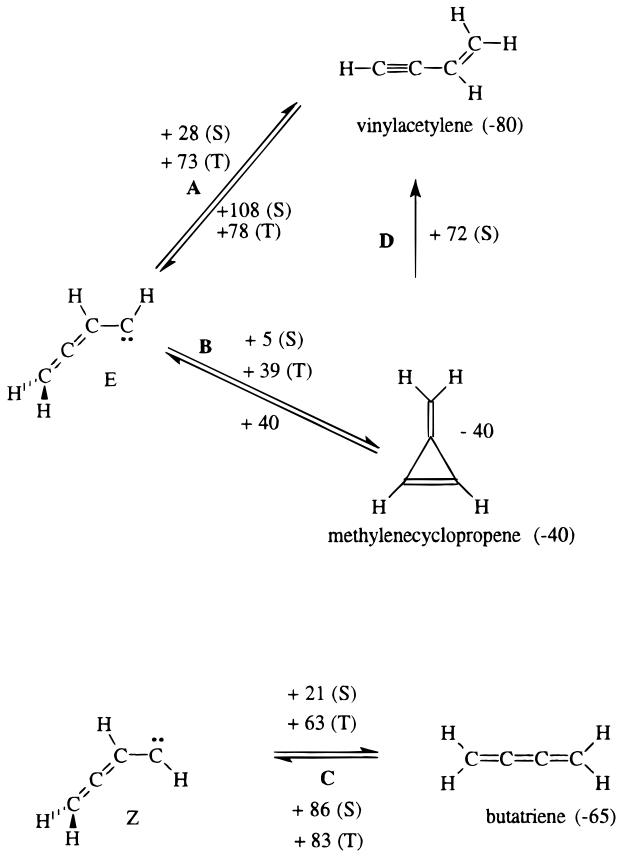

[a] Energies are in kilocalorie/mole.

In addition, observation of weak absorption bands at 1605 and 858 cm^{-1}, as for those recorded at 100 K for **6** by Miller and Matsubara[8b,] is compatible with the presence of a small amount of this compound.

Quantum Study of the Allenylcarbene Reactivity. *Structure of the Allenylcarbene Conformers.* Allenylcarbene may exist in two conformers Z and E, as triplets (hereafter referred as ^{3}Z and ^{3}E) or singlets (^{1}Z and ^{1}E) (Scheme 2). Four systems have been considered. In each case, the ground-state electronic configuration is highly multiconfigurational. As an example, the |222 000> determinant is attributed a weight in the CASSCF wave functions of 0.775 and 0.745, respectively, in ^{1}Z and ^{1}E. In the ^{3}E and ^{3}Z wave functions, the |221100> determinant has a coefficient of 0.690 and 0.702. These values are very small for ground states and the Hartree−Fock or Møller−Plesset reactivity calculations give completely erroneous results.

The optimized structures and associated energies are reported in Table 4. In relative energies, the triplets are more stable than the singlets by 10.6 kcal mol^{-1} for the Z form and 10.2 kcal mol^{-1} for the E form; the allenylcarbene ground state is therefore a triplet. The energy difference between ^{3}E and ^{3}Z is about 0.5 kcal mol^{-1}, 0.1 kcal mol^{-1} between the two singlets. Such narrow gaps are not significant, even at this stage of the theory. The consequence is that the structure parameters are also very similar, except for the fact that the θ_{734} angle is notably larger in ^{1}E than that in ^{1}Z due to the electrostatic repulsion between the lone pair of electrons borne by C_7 (which lies in the carbon chain plane) and the electronic density on C_4. In all cases, the ρ_{34} bond length is larger than those of ρ_{32} and ρ_{21}, indicating that the C_4 atom hybridization is intermediate between sp^2 and sp^3. This is important for the reactivity of the allenylcarbenes because along the different reaction pathways the structure of this atom continuously varies between various hybrid states inducing dramatic perturbations on the potential energy surfaces.

TABLE 4: Structure and Total Energy of the Allenylcarbene Conformers Z and E, Singlet and Triplet States[a]

parameters	^1E	^1Z	^3E	^3Z
ρ_{32}	1.333	1.332	1.345	1.345
ρ_{21}	1.310	1.313	1.315	1.315
ρ_{15}	1.075	1.075	1.077	1.077
ρ_{16}	1.075	1.075	1.077	1.077
ρ_{37}	1.080	1.080	1.080	1.078
ρ34	1.457	1.462	1.409	1.409
ρ_{48}	1.098	1.096	1.072	1.072
θ_{734}	124.5	118.9	117.5	117.6
θ_{348}	106.4	106.0	129.2	130.1
θ_{516}	118.3	118.2	117.1	117.2
τ_{5134}	89.6	89.7	90.0	89.8
E(CASSCF)	−153.676 910	−153.677 028	−153.693 111	−153.693 930

[a] Bond lengths in angstroms, angles in degrees, and energy in Hartrees.

Allenylcarbene Isomerization (Scheme 2). As shown in the previous section, the Z and E isomers are energetically equivalent irrespective of the spin multiplicity. As a consequence and due to the very large amount of calculation, only one of the two isomers' reactivity has been considered. The quantum study was carried out at the same level of theory as that of the structures. Each point of the PESs has been calculated separately, starting from the equilibrium structure of the preceding point on the same PES. No attempt at automatic gradient calculation for the transition states has been made because of the huge computation time it would require.

The allenylcarbenes are characterized by a lone pair of electrons on C_4. The migration of one of these electrons from C_4 to C_2 would lead to the biradical structure and transform the PES profiles. A similar problem was discussed by Cooksy[29] on nonequivalent canonical structures for a given radical corresponding to multiple minima. The possible transposition carbene ↔ biradical was studied for the two spin multiplicities and with ρ_{32} as the reaction coordinate. In the singlet PES, the migration reaction is quenched by cyclization, whereas in the triplet state, the energy of the system grows continuously with ρ_{32} without minimum. From these results, it may be inferred that the biradical structure is not stable and may be discarded from the possible reaction pathways. Nevertheless, along all the reaction paths, the C_4 atom structure can evolve very sharply, inducing dramatic effects in the PES calculation.

The isomerization reactions investigated in this work are displayed in Scheme 2, and only the cyclobutadiene target has not been considered because it is generally considered less probable. The PESs associated to the singlet isomerization are collected in Figure 7, and those associated to the triplet are shown in Figure 8. A and B reactions have been investigated starting from the E form, but it must be emphasized that the C reactions were carried out starting from the Z isomer because it was completely impossible to achieve the study with ^{3}E due to a great number of numerical instabilities in the CASSCF calculations.

The angle θ_{732} is the internal coordinate associated to reaction A (Figures 7A and 8A). Concerning the ^{1}E reaction, in the carbene, the CH_2 group is perpendicular to the carbon chain plane. The growth in energy in Figure 8A corresponds to the 90° rotation of this moiety, and the transition state displays a plane structure that also remains in the vinylacetylene. This

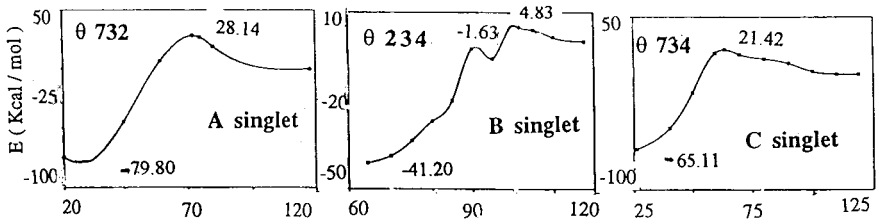

Figure 7. Potential energy surfaces for isomerization of the singlet allenylcarbene.

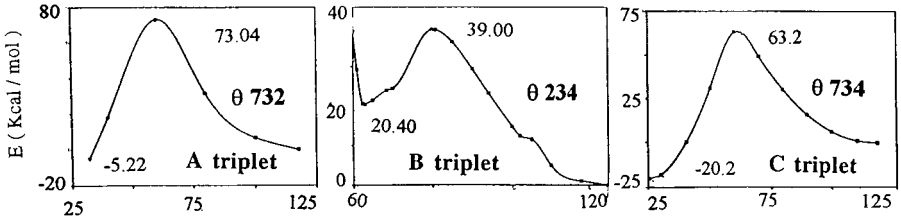

Figure 8. Potential energy surfaces for isomerization of the triplet allenylcarbene.

TABLE 5: Activation Energy Barriers (kcal mol^{-1}) for the Isomerization Reactions of Allenylcarbene Z for Reactions A and B and E for Reaction C (Figure 2)

	singlet	triplet
	Z	
A	28.1	73.0
B	4.8	39.0
	E	
C	21.4	63.0

rotation is also accompanied by an increase of the ρ_{32} bond length, which evolves from 1.341 to 1.477 Å in TS before it then decreases down to 1.435 Å; the associated activation energy barrier is illustrated in Table 5.

Figure 7B shows a rather unusual aspect with a relative minimum. The associated reaction coordinate is θ_{234}. In the singlet the CH_2 moiety remains perpendicular to the chain plane until the first maximum is reached (relative energy 4.83 kcal mol^{-1}). The second maximum (relative energy −1.63 kcal mol^{-1}) corresponds to a plane structure that is preserved until cyclization. ρ_{32} grows from 1.457 to 1.461 Å for TS and then decreases to 1.318 Å in methylenecyclopropene.

The coordinate associated to reaction C is θ_{734}. The Schlegel algorithm, although much longer in computational time, was successfully carried out in order to reach convergence during the geometry optimizations.

The activation energy barriers associated with the triplet are always significantly higher than those of the singlets (Table 5). In the singlet wave functions, the free electrons are paired and the lone pair is located in either a chain or perpendicular plane. The electronic interactions can be minimized by the transfer of the pair from one situation to the other. On the contrary, in the triplet, one of the electrons is always in the plane, and the wave function of the second is always perpendicular; as a consequence, whatever the spatial structure, at least one of the two is in a destabilizing situation and the transition barrier is higher. Figures 9 and 10 indicate that when the TS associated with the singlet is planar, the TS associated to the triplet has a nonplanar structure. This is also observed for the final products concerning the vinylacetylene, which is planar only in the singlet state, and the butatriene, which is twisted as a triplet and planar as a singlet.

The singlet reactions are always exothermic (40−80 kcal mol^{-1}), whereas the triplet reactions are noticeably less stabilizing because the gains in energy from the initial to the final state ranges from 5 to 20 kcal mol^{-1}; the triplet isomerization leading

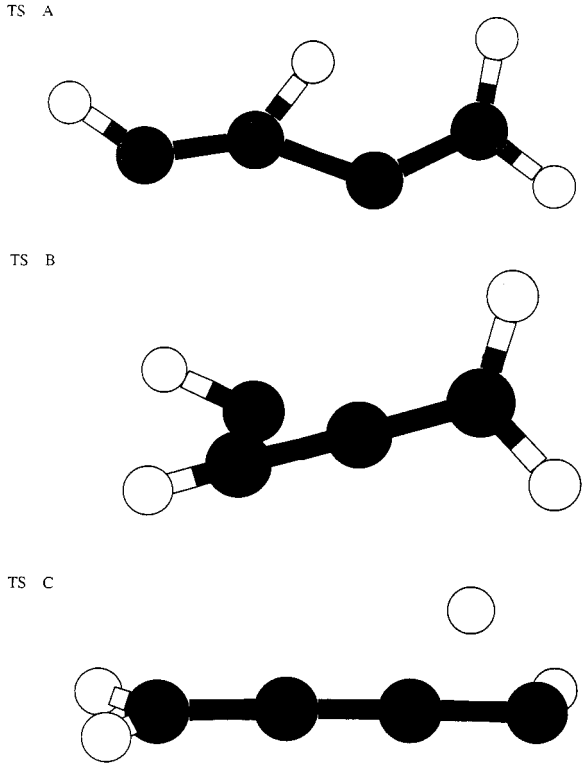

Figure 9. Structure of the transition states corresponding to the potential energy surfaces of isomerization of the singlet allenylcarbene.

to cyclopropene is even endothermic because the molecule is less stable than the carbene. The structures and energies of the final products are reported in Table 6.

Methylenecyclopropene → Vinylacetylene Interconversion. The interconversion of singlet-state methylenecyclopropene to vinylacetylene has also been studied. The two-dimensional PES (Figure 11) has been drawn considering the C4−C2 distance and the C2−C3−H7 angle as the first and the second variable, respectively. The reaction path runs from the upper left corner (1.4738 Å, 147.7°) to the point representing the plane form of vinylacetylene (2.45 Å, 35°). The saddle point is 72.2 kcal mol^{-1} above the starting point.

Acetylene Formation. Acetylene was assumed to be a product of photolysis of **3**. Then, its formation from **3** has also been investigated in both singlet and triplet cases. The coordinate associated to the reaction is the single CC bond ρ_{12}. Opposition to that could have been expected: only the H6 hydrogen

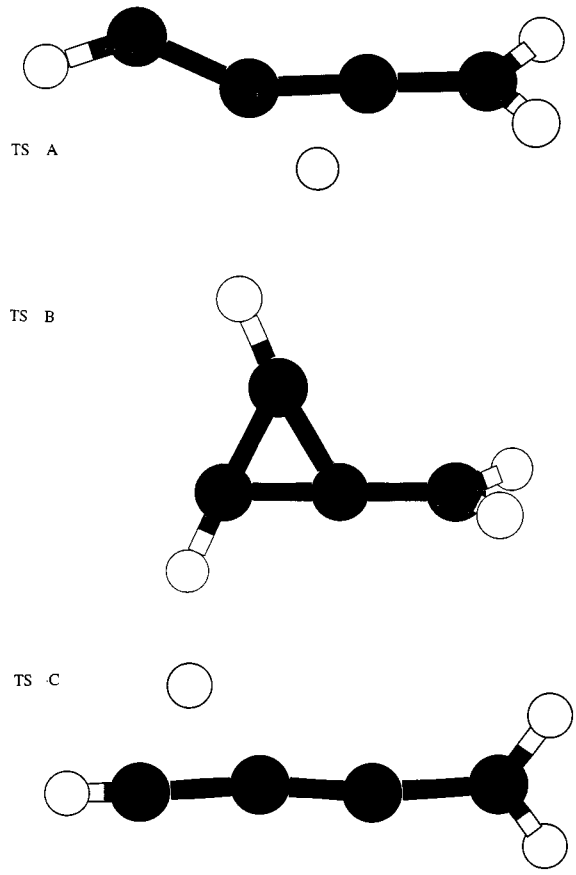

Figure 10. Structure of the transition states corresponding to the potential energy surfaces of isomerization of the triplet allenylcarbene.

TABLE 6: Structure and Energy (relative to the implicated carbene) of the Final Product of Reactions A to C[a]

parameters	^{1}**4**	^{3}**4**	^{1}**5**	^{3}**5**	^{1}**6**	^{3}**6**
ρ_{32}	1.440	1.373	1.446	1.358	1.267	1.233
ρ_{21}	1.343	1.469	1.331	1.414	1.332	1.397
ρ_{15}	1.074	1.072	1.074	1.072	1.075	1.397
ρ_{16}	1.074	1.076	1.074	1.072	1.075	1.073
ρ_{37}	1.076	1.092	1.068	1.062	1.075	1.073
ρ_{34}	1.211	1.220	1.315	1.358	1.332	1.397
ρ_{48}	1.056	1.056	1.068	1.062	1.075	1.073
θ_{734}	120.0	121.9	148.4	151.0	121.2	120.8
θ_{348}	180.0	180.0	148.4	151.0	121.2	120.8
θ_{516}	117.4	118.2	117.9	118.9	117.6	118.5
τ_{5134}	0	109.2	0	0	0	90.3
E (relative)	−79.8	−5.2	−41.2	20.4	−65.1	−20.2

[a] Bond lengths in angstroms, angles in degrees, and energy in kcal mol^{-1}.

rearranges during the process and migrates to C7, thus then leading to **6**. Afterward, the butatriene molecule breaks into two vinylidene radicals H2CC**:** with associated barriers of 110 and 124 kcal mol^{-1} for the singlet and the triplet states, respectively. Such values are consistent with the breaking of double bonds and the photon energy.

Then, the singlet vinylidene yields acetylene. The value of the calculated reaction barrier, 5.4 kcal mol^{-1}, is similar to those previously predicted.[31] As previously reported,[32] the triplet vinylidene and the trans isomer of acetylene have nearly the same total energy. The energy barrier between these two species is 70.7 kcal mol^{-1}. It is well-established that in its triplet state the acetylene molecule is mostly in a cis-bent conformation, but the energy difference between the cis-bent and the trans-bent forms (5.3 kcal mol^{-1}) cannot alter the present results significantly.

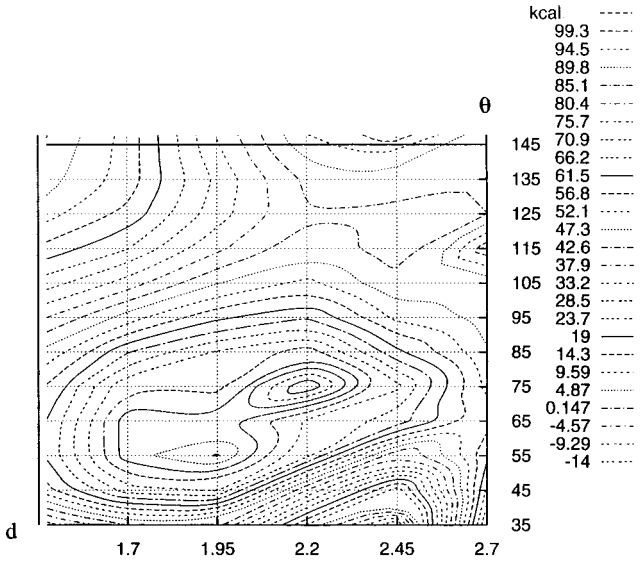

Figure 11. Potential energy surfaces of the interconversion of **5** to **4**.

The acetylene moieties trapped in the same cage can yield dimers. These clusters are characterized by absorption bands in the 3279−3285 cm^{-1} area.[33]

Conclusion

The equilibrium structure and thermodynamic stabilities of the four isomers of C_4H_4 have been computed at the LSDA/6-31G** level of theory. The calculations suggest that singlet **4** is the minimum (−80 kcal mol^{-1}). Calculated activation barriers for **3** isomerization reaction paths are very low (Table 5), and formation of methylenecyclopropene **5** is the more favorable process (5 kcal mol^{-1}). Then, the evolution of the 1770 cm^{-1} absorption band shows that **5** is an intermediate that isomerizes in **4** under UV irradiation.[8b] Photodissociation of **3** leads vinylidene transients that isomerize in acetylene **7**.

Registry Numbers

Allenylketene (**2**) 156495-78-2, vinylacetylene (**4**) 689-97-4, methylenecyclopropene (**5**) 4095-06-1, butatriene (**6**) 2873-50-9, and acetylene (**7**) 74-86-2. Registry numbers have been supplied by the author.

Acknowledgment. M.H. thanks the French "Ministère des Affaires Étrangères" and the Town Hall of Marseilles for a grant. The CNRS (Institut du developpement et des ressources en Informatique Scientifique) is gratefully acknowledged for their financial support.

Supporting Information Available: Optimized geometric molecular parameters (LSDA/6-31G**) of the two conformers of 3,4-pentadienoyl chloride and the two conformers **2** *s*-E and **2** *s*-E, LSDA/6-31G** optimized structure and atom numbering of the two conformers of 3,4-pentadienoyl chloride and the two conformers **2** s−E and **2** s−Z, and the butatriene-to-vinylidene and the vinylidene-to-acetylene reactions (both with PES associated to both the singlet and the triplet states).

References and Notes

(1) (a) Kirmse, W. *Carbene Chemistry*, 2nd ed.; Academic Press: New York, 1971. (b) Moss, R. A.; Jones, M., Jr. *Carbenes;* Wiley: New York, 1973; Vol. 1. Jones, M., Jr.; Moss, R. A. *Carbenes*; Wiley: New York, 1975; Vol. 2. (c) Wentrup, C. *Reactive Molecules: The Neutral Reactive Intermediates in Organic Chemistry*; Wiley: New York, 1984.

(2) McKellar, A. R. W.; Bunker, P. R.; Sears, T. J.; Evenson, K. M.; Saykally, R. J.; Langhoff, S. R. *J. Chem. Phys.* **1983**, *79*, 5251.

(3) Liebman, J. F.; Simons, J. *Molecular Structure and Energetics*; V. C. H. Publishers Inc.: Deerfield Beach, FL, 1986; Vol. 1, p 92.

(4) Greenberg, A.; Liebman, J. F. *Strained Organic Molecules*; Academic Press: New York, 1978; pp 93−95, 240−243, and 274−276.

(5) (a) Thaddeus, P.; Vrtilek, J. M.; Gottlieb, C. A. *Astrophys. J.* **1985**, *299*, L63. (b) Adams, N. G.; Smith, D. *Astrophys. J.* **1987**, *317*, L25. (c) Gottlieb, C. A.; Killian, T. C.; Thaddeus, P.; Bostchwina, P.; Flügge, J.; Oswald, M. *J. Chem. Phys.* **1993**, *98*, 4478. (d) Seburg, R. A.; McMahon, R. J.; Stanton, J. F.; Gauss, J. *J. Am. Chem. Soc.* **1997**, *119*, 10838.

(6) (a) Maier, G.; Reisenauer, H. P.; Schawb, W.; Carsky, P.; Hess, B. A.; Schaad, L. J. *J. Am. Chem. Soc.* **1987**, *109*, 5183. (b) Maier, G.; Reisenauer, H. P.; Schawb, W.; Carsky, P.; Spirko, V.; Hess, B. A.; Schaad, L. J. *J. Chem. Phys.* **1989**, *91*, 4763. (c) Jonas, V.; Böhme, M.; Frenking, G. *J. Phys. Chem.* **1992**, *96*, 1640.

(7) (a) Coffman, D. D. *J. Am. Chem. Soc.* **1935**, *57*, 1978. (b) Tørneng, E.; Nielsen, C. J.; Klaboe, P.; Hopf, H.; Priebe, H. *Spectrochim. Acta* **1980**, *36A*, 975. (c) Walch, S. P.; Taylor, P. R. *J. Chem. Phys.* **1995**, *103*, 4975. (d) Hofmann, J.; Zimmermann, G.; Findeisein, M. *Tetrahedron Lett.* **1995**, *36*, 3831. (e) Sheppard, N. *J. Chem. Phys.* **1949**, *17*, 74.

(8) (a) Schubert, W. M.; Liddicoet, T. H.; Lanka, W. A. *J. Am. Chem. Soc.* **1954**, *76*, 1929. (b) Miller, F. A.; Matsubara, I. *Spectrochim. Acta* **1966**, *22*, 173. (c) Stoicheff, B. P. *Can. J. Phys.* **1957**, *35*, 837.

(9) (a) Chapman, O. L.; McIntosh, C. L.; Pacansky, J. *J. Am. Chem. Soc.* **1973**, *95*, 244. (b) Chapman, O. L.; McIntosh, C. L.; Pacansky, J. *J. Am. Chem. Soc.* **1973**, *95*, 614.

(10) (a) Fitzgerald, D.; Saxe, P.; Schaefer, H. F., III. *J. Am. Chem. Soc.* **1983**, *105*, 690. (b) Carlson, H. A.; Quelch, G. E.; Schaefer, H. F., III. *J. Am. Chem. Soc.* **1992**, *114*, 5344. (c) Johnson, R. P.; Daoust, K. J. *J. Am. Chem. Soc.* **1995**, *117*, 362. (d) Gilbert, J. C.; Kirschner, S. *Tetrahedron* **1996,** *52*, 2279**.**

(11) (a) Billups, W. E.; Lin, L. J.; Casserly, E. W. *J. Am. Chem. Soc.* **1984**, *106*, 3698. (b) Staley, S. W.; Norden, T. D. *J. Am. Chem. Soc.* **1984**, *106*, 3699. (c) Hess, B. A.; Michalska, D.; Schaad, L. J. *J. Am. Chem. Soc.* **1985**, *107*, 1449. (d) McAllister, M. A.; Tidwell, T. T. *J. Am. Chem. Soc.* **1992**, *114*, 5362. (e) Langler, R. F.; Precedo, L. *Can. J. Chem.* **1990**, *68*, 939. (f) Cioslowski, J.; Hamilton, T.; Scuseria, G.; Hess, B. A.; Hu, J.; Schaad, L. J.; Dupuis, M. *J. Am. Chem. Soc.* **1990**, *112*, 4183.

(12) (a) Huang, W.; Fang, D.; Temple, K.; Tidwell, T. T. *J. Am. Chem. Soc.* **1997**, *119*, 2832. (b) Chapman, O. L. *Pure Appl. Chem.* **1979**, *51*, 331. (c) Trahanovsky, W. S.; Park, M. K. *J. Am. Chem. Soc.* **1973**, *95*, 5412.

(13) (a) Bachmann, C.; N′Guessan, T. Y.; Debu, F.; Monnier, M.; Pourcin, J.; Aycard, J.-P.; Bodot, H. *J. Am. Chem. Soc.* **1990**, *112*, 7488. (b) Risi, F.; Pizzala, L.; Carles, M.; Verlaque, P.; Aycard, J.-P. *J. Org. Chem.* **1996**, *61*, 666. **(**c) Piétri, N.; Chiavassa, T.; Allouche, A.; Aycard, J.-P. *J. Phys. Chem. A* **1997**, *101*, 1093. (d) Monnier, M.; Allouche, A.; Verlaque, P.; Aycard, J.-P. *J. Phys. Chem.* **1995**, *99*, 5977. (e) Piétri, N.; Chiavassa, T.; Allouche, A.; Rajzmann, M.; Aycard, J.-P. *J. Phys. Chem.* **1996**, *100*, 7034.

(14) Kogure, N.; Ono, T.; Suzuki, E.; Watari, F. *J. Mol. Struct.* **1993,** *296*, 1.

(15) Price, T. A.; Patten, T. E. *J. Chem. Educ.* **1991**, *68*, 256.

(16) Hb(Hb′)C═C═CHcCHa(Ha)COCl (solvent CCl_4, δ in ppm from TMS, J in Hz): $\delta_a = 3.58$, $\delta_{bb'} = 4.86$, $\delta_c = 5.25$; $J_{ab} = 2.7$, $J_{ab'} = 2$, 5, $J_{ac} = 7.1$, $J_{bc} = 6.2$, $J_{b'c} = 7.8$. These results are in good agreements with those of 3,4-pentadienoic acid.[15]

(17) Vosko, S. H.; Wilk, L.; Nusair, M. *Can. J. Phys.* **1980**, *58*, 1200.

(18) (a) Ditchfield, R.; Hehre, W. J.; Pople, J. A. *J. Chem. Phys.* **1971**, *54*, 724. (b) Hehre, W. J.; Ditchfield, R.; Pople, J. A. *J. Chem. Phys.* **1972**, *56*, 2257.

(19) (a) Roos, B. O. In *Methods in Computational Molecular Physics*; Diercksen, G. H. F., Wilson, S., D., Eds.; Reidel Publishing, Dordrecht, The Netherlands, 1983; p 61. (b) Werner, M. W. In *Advances in Chemical Physics*; Lawley, K. P., Ed.; Wiley Interscience: New York, 1987; Vol. 69, p 1. (c) Shepard, R. In *Advances in Chemical Physics*; Lawley, K. P., Ed.; Wiley-Interscience: New York, 1987; Vol. 69, p 63.

(20) Schmidt, M. W.; Baldridge, K. K.; Boatz, J. A.; Elbert, S. T.; Gordon, M. S.; Jensen, J. H.; Koseki, S.; Matsunaga, N.; N′Guyen, K. A.; Su, S. J.; Windus, T. L.; Dupuis, M.; Montgomery, J. A. *J. Comput. Chem.* **1993**, *14*, 1347.

(21) (a) Schlegel, H. B. *J. Comput. Chem.* **1982**, *3*, 214. (b) Schlegel, H. B. In *Advances in Chemical Physics*: *Ab Initio Methods in Quantum Chemistry*, Part I; Lawley, K. P., Ed.; Wiley-Interscience: New York, 1987; Vol. 67, p 249. (c) Schlegel, H. B. *Int. J. Quantum Chem.; Symp.* **1992**, *26*, 253.

(22) Chouteau, J.; Davidovics, G.; Bertrand, M.; Legras, J.; Figarella, J.; Santelli, M. *Bull. Soc. Chim. Fr.* **1964**, 2562.

(23) (a) Girardet, C.; Lakhlifi, A.; Laroui, B. *J. Chem. Phys.* **1992**, *97*, 7955. (b) Laroui, B.; Damak, O.; Maillard, O.; Girardet, C. *J. Chem. Phys.* **1992**, *97*, 2359. (c) Laroui, B.; Perchard, J.-P.; Girardet, C. *J. Chem. Phys.* **1992**, *97*, 2347. (d) Andrews, L.; Hunt, R. D. *J. Chem. Phys.* **1988**, *89*, 3502.

(24) Dewar, M. J. S.; Zoebisch, E. G.; Healy, E. F.; Stewart, J. J. P. *J. Am. Chem. Soc.* **1985**, *107*, 3902.

(25) Andrews, L.; Johnson, G. L.; Kelsall, B. *J. Phys. Chem.* **1982**, *86*, 3374.

(26) Tang, T. T.; Cui, Y. P. *Can. J. Chem.* **1996**, *74*, 1162.

(27) Kisiel, Z.; Fauler, P. C.; Legon, A. C.; Devanne, D.; Dixneuf, P. *J. Chem. Phys.* **1990**, *93*, 6249.

(28) Banert, K.; Hagedorn, M.; Knözinger, E.; Becker, A.; Würthwein, E. U. *J. Am. Chem. Soc.* **1994**, *116*, 60.

(29) Cooksy, A. L. *J. Am. Chem. Soc.* **1995**, *117*, 7, 1098.

(30) Ramsey, J. A.; Ladd, J. A. *J. Chem. Soc. (B)* **1968**, 120.

(31) In the most complete ab initio study, Gallo et al.,[31d] predicted 3 kcal. mol^{-1} for the classical barrier, with became 1.6 $kcal.mol^{-1}$ when zero-point vibrational energy was taken into account. (a) Osamura, Y.; Schaefer, H. F.; Gray, S. K.; Miller, W. H. *J. Am. Chem. Soc.* **1981**, *103*, 3, 1904. (b) Krishnan, R.; Frisch, M. J.; Pople, J. A.; Schleyer, P. v. R. *Chem. Phys. Lett.* **1981**, *79*, 408. (c) Carrington, T.; Hubbard, L. M.; Schaefer, H. F., III; Miller, W. H. *J. Chem. Phys.* **1984**, *80*, 4347. (d) Gallo, M. M.; Hamilton, T. P.; Schaefer, H. F., III. *J. Am. Chem. Soc.* **1990**, *112*, 8714.

(32) Allouche, A. *J. Phys. Chem.* **1996**, *100*, 17915.

(33) Prichard, D. G.; Nandi, R. N.; Muenter, J. S. *J. Chem. Phys.* **1988**, *89*, 115.